Supporting Information

Cross-stacked Superaligned Carbon Nanotube Electrode for Efficient Hole Conductor-free Perovskite Solar Cells

Qiang Luo,[a,†] He Ma,[b,†] Ye Zhang,[a] Xuewen Yin,[a] ZhiBo Yao,[a] Ning Wang,[c] Jianbao Li,[a,d] Shoushan Fan,[b] Kaili Jiang,[b,*] Hong Lin,[a,*]

[a] State Key Laboratory of New Ceramics & Fine Processing, School of Material Science and Engineering, Tsinghua University, Beijing 100084, China
[b] State Key Laboratory of Low-Dimensional Quantum Physics, Tsinghua-Foxconn Nanotechnology Research Center, Department of Physics, Collaborative Innovation Center of Quantum Matter, Tsinghua University, Beijing 100084, China
[c] College of Materials Science and Chemical Engineering, Hainan University, Haikou 570228, China
[d] State Key Laboratory of Electronic Thin Films and Integrated Devices, University of Electronic Science and Technology of China, Chengdu 610054, China
† These authors contributed equally to this work

Corresponding Author

*hong-lin@mail.tsinghua.edu.cn

*JiangKL@mail.tsinghua.edu.cn

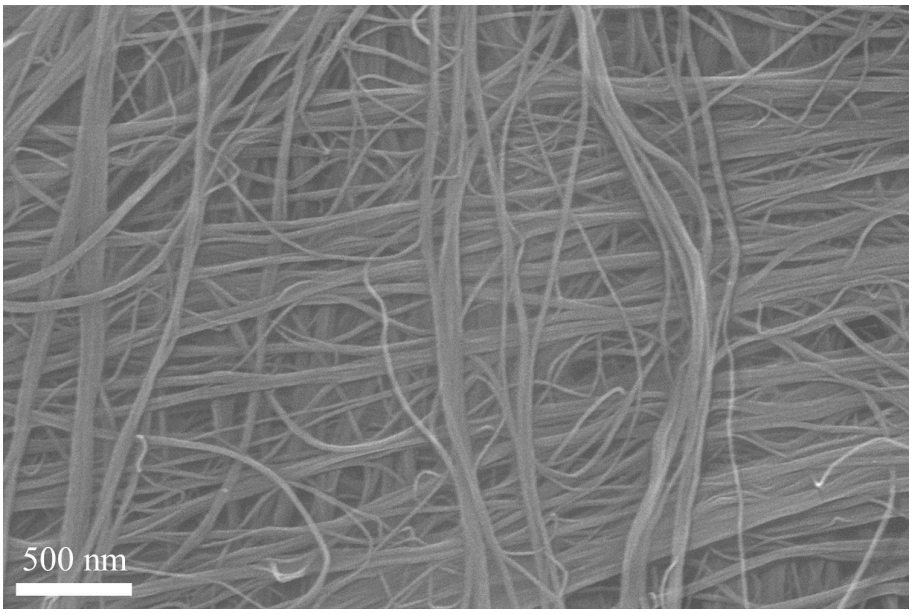

Figure S1. SEM image of T-CSCNT-50.

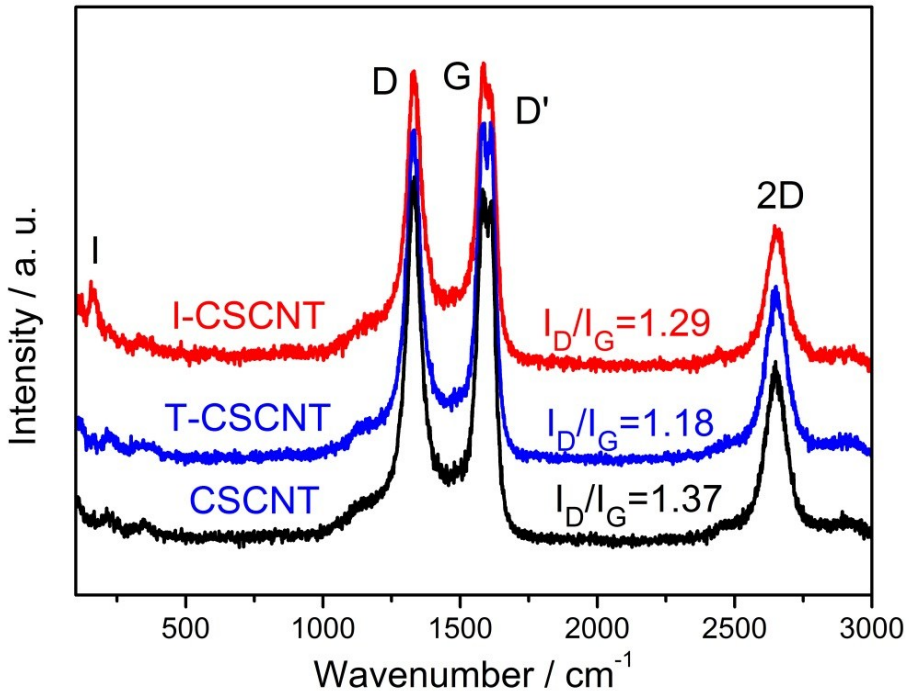

Figure S2. Raman spectra of CSCNT-50, T-CECNT-50 and I-CSCNT-50. The I_D/I_G ratio of I-CSCNT (1.29) was much lower than that of CSCNT (1.37), demonstrating a lower density of defect sites due to the iodine doping. The Raman peaks at 155 cm^{-1} can be assigned to iodine doping.

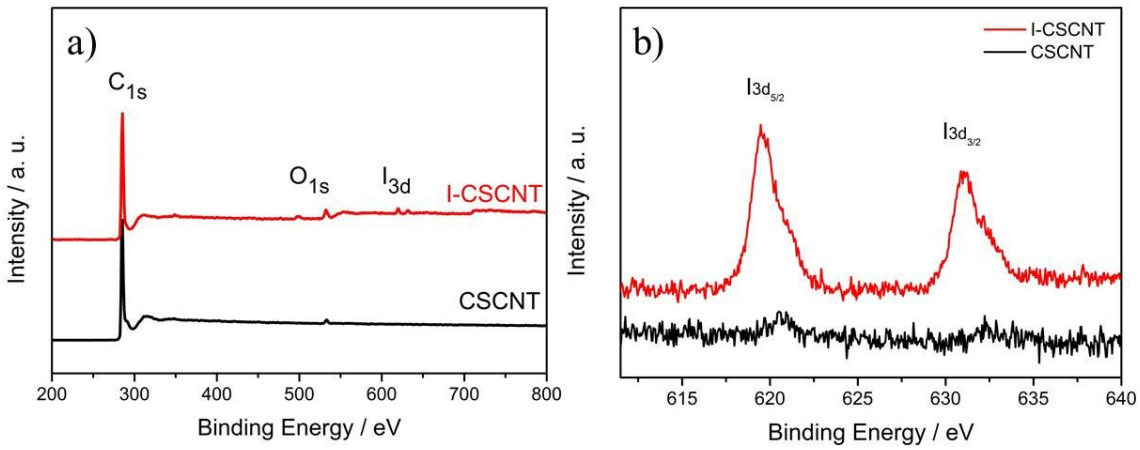

Figure S3. (a) XPS survey spectra and (b) high-resolution I3d spectra of CSCNT and I-CSCNT.

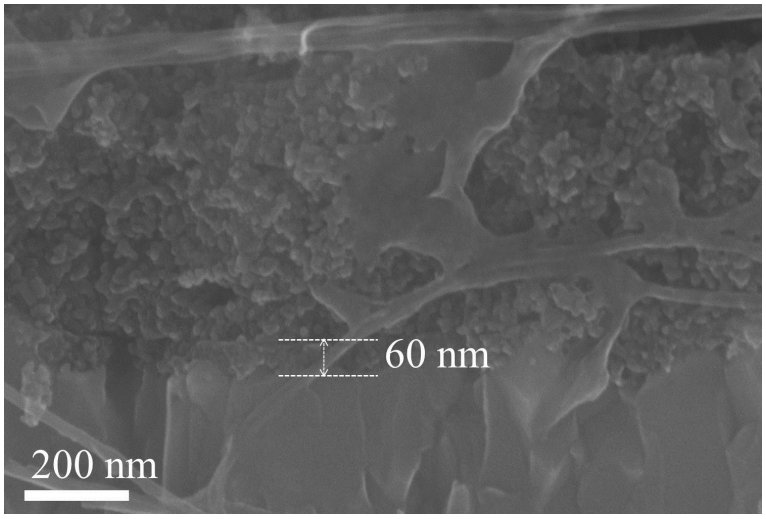

Figure S4. Typical cross-sectional image of the FTO/compact TiO_2 layer/ mesoporous TiO_2 layer in a PSC.

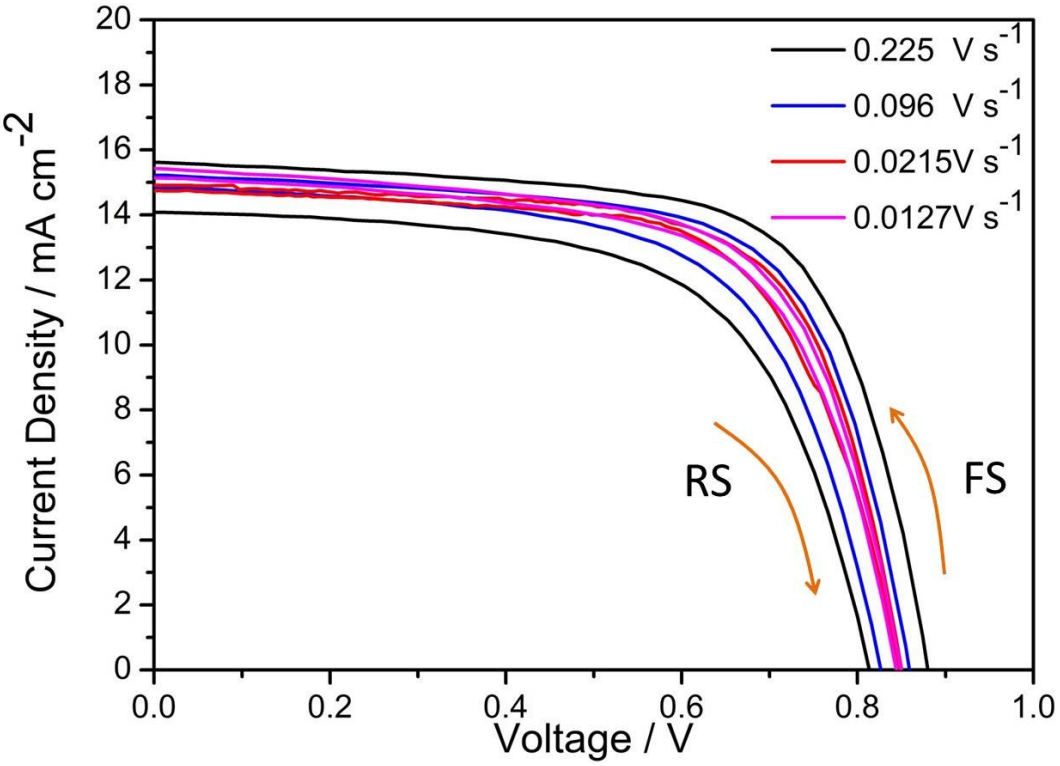

Figure S5. The *J-V* curves of CSCNT-50-based PSC with different scan directions and rates.

Table S1. Photovoltaic parameters of CSCNT-50 based PSCs with different scan directions and scan rates under simulated AM1.5, 100 mW cm^{-2} solar irradiation.

Scan rate [V s^{-1}]	Scan directions	V_{oc} [mV]	J_{sc} [mA cm^{-2}]	FF	PCE [%]
0.225	FS	873	15.60	0.683	9.327
	RS	805	14.09	0.634	7.136
0.096	FS	854	15.21	0.678	8.822
	RS	820	14.83	0.638	7.727
0.0313	FS	854	15.22	0.678	8.812
	RS	836	15.03	0.658	8.268
0.0215	FS	850	14.91	0.678	8.602
	RS	840	14.75	0.665	8.265
0.0127	FS	852	15.31	0.670	8.720
	RS	840	15.13	0.660	8.390

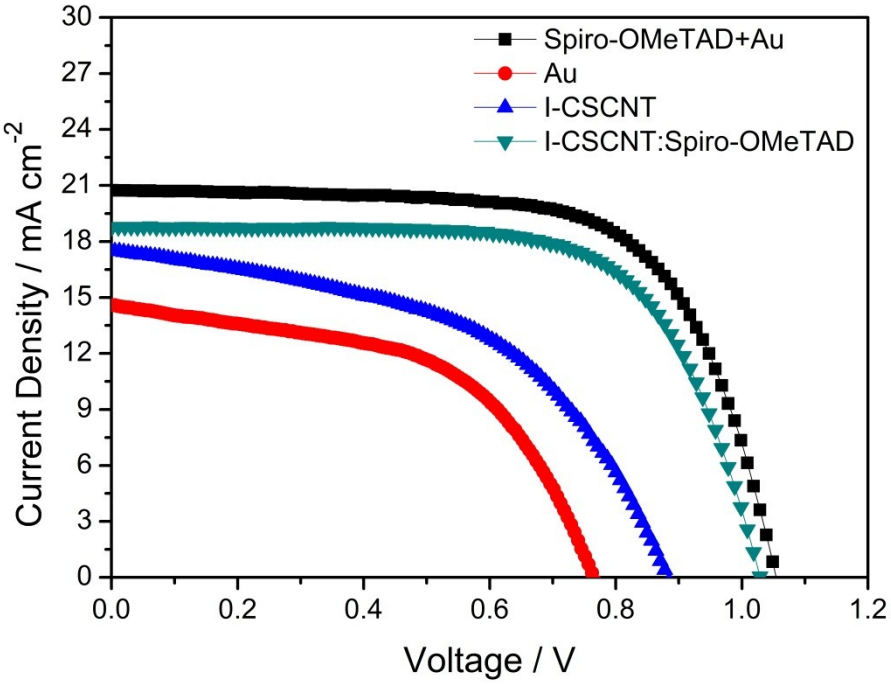

Figure S6. The *J-V* curves of standard PSCs with the spin-coated spiro-OMeTAD HTM and evaporated gold back contact and I-CSCNT-based PSCs with spiro-OMeTAD HTM (FTO/TiO_2/perovskite/spiro-OMeTAD/I-CSCNT) and without spiro-OMeTAD HTM (FTO/TiO_2/perovskite/I-CSCNT).

Table S2. Photovoltaic parameters of standard PSCs under simulated AM1.5, 100 mW cm^{-2} solar irradiation.

Samples	V_{oc} [mV]	J_{sc} [mA cm^{-2}]	FF	PCE [%]
Spiro-OMeTAD+Au	1050	20.74	0.68	14.76
Au	763	14.58	0.53	5.92
I-CSCNT-50	880	17.48	0.50	7.70
Spiro-OMeTAD+I-CSCNT-50	1030	18.78	0.68	13.12

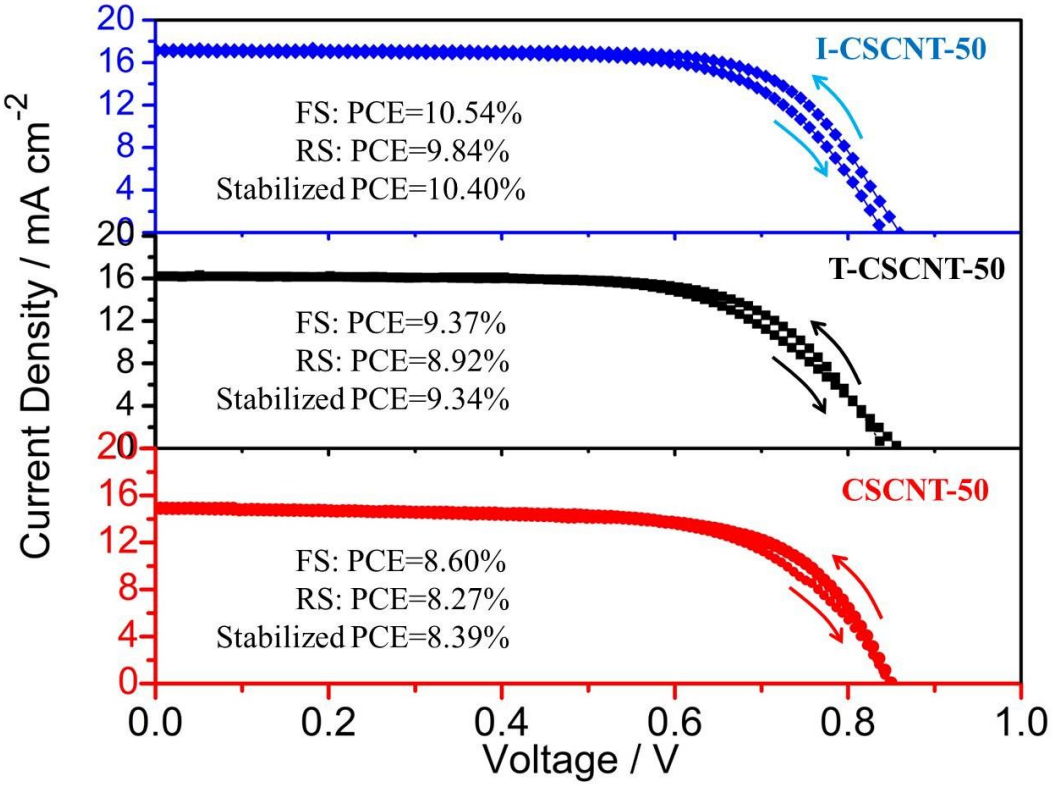

Figure S7. The *J-V* curves of different PSCs with different scan directions at a rate of 0.0215 V s^{-1}.

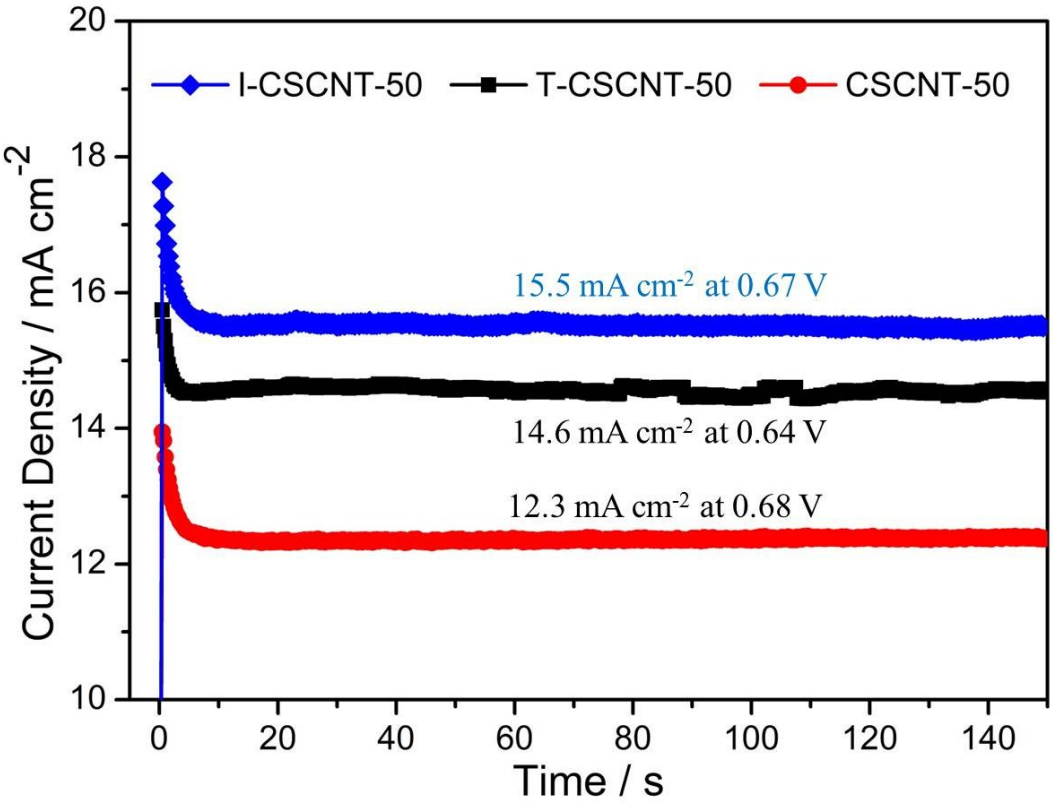

Figure S8. The photocurrent density as a function of time for the cells held at a forward bias of maximum output power point (0.64, 0.67, and 0.68 V for the devices based on T-CSCNT-50, I-CSCNT-50 and CSCNT-50, respectively).

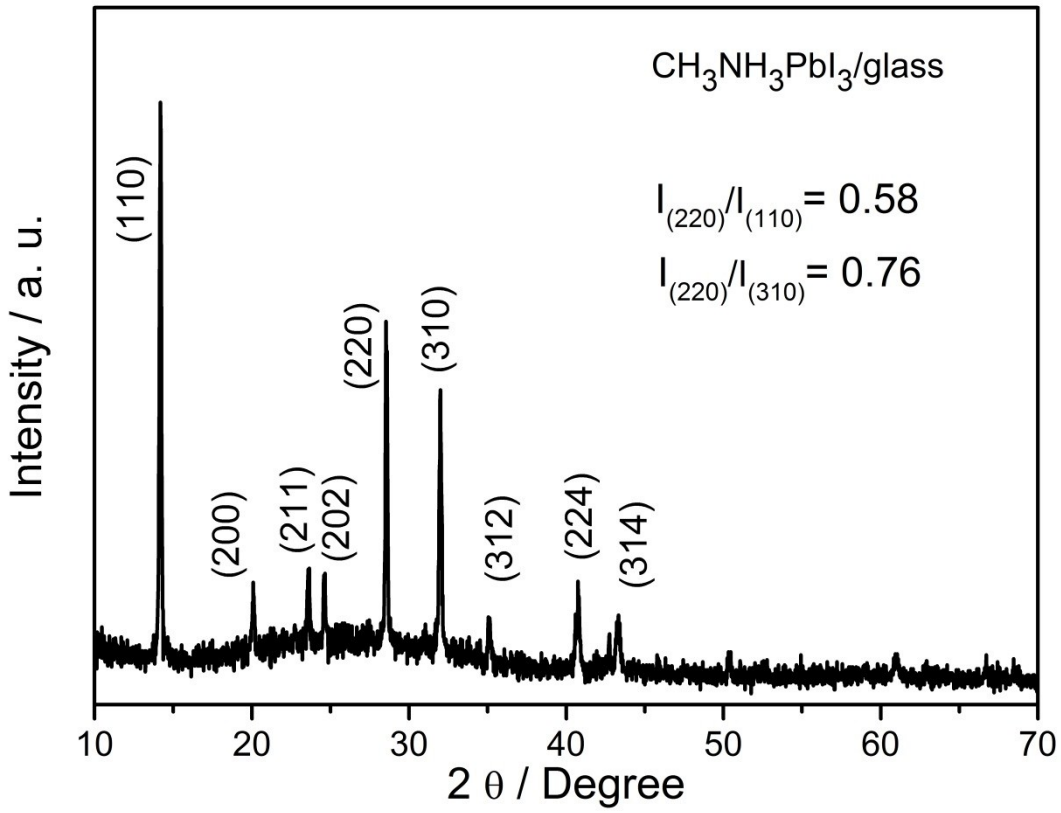

Figure S9. XRD pattern of the $CH_3NH_3PbI_3$ perovskite deposited on glass